Journal of Fluorescence, Vol. 16, No. 1, January 2006 (© 2006)
DOI: 10.1007/s10895-005-0043-y

Upconversion Properties of Er^{3+}/Yb^{3+} Co-doped TeO_2–TiO_2–K_2O Glasses

Fangning Su[1,2] and Zaide Deng[1]

Received October 16, 2005; accepted November 22, 2005
Published online: January 6, 2006

The Er^{3+}/Yb^{3+} co-doped TeO_2–TiO_2–K_2O glasses were prepared by conventional melting procedures, and their upconversion spectra were performed. The dependence of luminescence intensity on the ratio of Yb^{3+}/Er^{3+} was studied, and the relationship between green upconversion luminescence intensity and Er^{3+} concentration is discussed in detail. The 546 nm green upconversion luminescence intensity is optimised in the studied glasses either when the Yb^{3+}/Er^{3+} ratio is 25/1 and Er^{3+} concentration is 0.1 mol%, or when the Yb^{3+}/Er^{3+} ratio is 10/1 and Er^{3+} concentration is 0.15 mol%. These glasses could be one of the potential candidates for LD pumping microchip solid-state lasers.

KEY WORDS : Upconversion; Rare earth ions; Tellurite glasses.

INTRODUCTION

Upconversion properties of rare earth ions-doped glasses have attracted much attention in resent years due to their excellent optical properties. These materials have potential applications in the information process, data storage, display technology, undersea transmission, and medicine [1–6]. Particularly, tellurite glasses have been investigated extensively because of their relative low phonon energy, high refractive index, good corrosion resistance, and high thermal stability.

Er^{3+}/Yb^{3+} co-doped glasses [7,8] are attractive because Yb^{3+} has excellent absorption efficiency [9] at 976 nm, and Er^{3+} possesses an intermediate level ($^4I_{11/2}$) with long life-time. This work is to study the influence of Er^{3+} concentration and the Er^{3+}/Yb^{3+} ratio in tellurite glasses on the 546 nm green upconversion luminescence intensity, and to find out better candidate for the microchip short wavelength lasers.

The compositions of the Er^{3+}/Yb^{3+} co-doped tellurite glasses are shown in Table I. Their absorption and upconversion spectra were measured. Two green emission bands centred at 523 and 547 nm, corresponding to the $^2H_{11/2}\rightarrow{}^4I_{15/2}$ and $^4S_{3/2}\rightarrow{}^4I_{15/2}$ transitions, respectively, and one red emission band centred at 657 nm by $^4F_{9/2}\rightarrow{}^4I_{15/2}$ transition, were observed. The dependence of luminescence intensity on the ratio of Yb^{3+}/Er^{3+} and Er^{3+} concentration are discussed in detail.

EXPERIMENTS

Glasses Preparation

All starting materials for Er^{3+}/Yb^{3+} co-doped glasses are analytical grade chemicals of TeO_2, TiO_2, K_2CO_3, Er_2O_3, and Yb_2O_3. The glasses base compositions (in mol%) are $80TeO_2$–$(10-\chi-\chi R)TiO_2$–$10K_2O$–χEr_2O_3–$\chi R Yb_2O_3$ ($\chi = 0.1$, 0.15, 0.2, 0.25, 0.3, 0.4, 0.5, and 1.0; R, the ratio of Yb^{3+}/Er^{3+}, $R = 1/10$, 1/5, 1/4, 1/3, 1/2, 1/1, 2/1, 3/1, 4/1, 5/1, 10/1, 15/1, 20/1, 25/1, 30/1, and 35/1), and the studied compositions are listed in Table I.

The well-mixed batches were melt in Pt crucible at 850°C for 30 min in an electric furnace, then the glasses were poured into a stainless steal mould and annealed in a

[1] Institute of Optical Communication Materials, College of Materials Science and Engineering, South China University of Technology, Guangzhou, 510640, PR China.
[2] To whom correspondence should be addressed. E-mail: sufangning-2003@etang.com

Table I. The Glasses Compositions (in Molar Percentage)

Sample no	TeO_2	K_2O	TiO_2	Er_2O_3	Yb_2O_3	χ	R
Series I							
TTK-1-1	80	10	8.9	1.0	0.1	1.0	1/10
TTK-1-2	80	10	9.4	0.5	0.1	0.5	1/5
TTK-1-3	80	10	9.5	0.4	0.1	0.4	1/4
TTK-1-4	80	10	9.6	0.3	0.1	0.3	1/3
TTK-1-5	80	10	9.7	0.2	0.1	0.2	1/2
TTK-1-6	80	10	9.8	0.1	0.1	0.1	1/1
TTK-1-7	80	10	9.7	0.1	0.2	0.1	2/1
TTK-1-8	80	10	9.6	0.1	0.3	0.1	3/1
TTK-1-9	80	10	9.5	0.1	0.4	0.1	4/1
TTK-1-10	80	10	9.4	0.1	0.5	0.1	5/1
TTK-1-11	80	10	8.9	0.1	1.0	0.1	10/1
Series II							
TTK-2-1	80	10	8.9	0.1	1.0	0.1	10/1
TTK-2-2	80	10	8.4	0.1	1.5	0.1	15/1
TTK-2-3	80	10	7.9	0.1	2.0	0.1	20/1
TTK-2-4	80	10	7.4	0.1	2.5	0.1	25/1
TTK-2-5	80	10	6.9	0.1	3.0	0.1	30/1
TTK-2-6	80	10	6.4	0.1	3.5	0.1	35/1
TTK-2-7	80	10	8.35	0.15	1.5	0.15	10/1
TTK-2-8	80	10	7.8	0.2	2.0	0.2	10/1
TTK-2-9	80	10	7.25	0.25	2.5	0.25	10/1
TTK-2-10	80	10	6.7	0.3	3.0	0.3	10/1

muffle oven at their T_g points. The annealed glasses were cut into 15 mm × 15 mm × 1.5 mm pieces and then polished for optical measurements.

Properties Measurements

The absorption spectra of the glass samples were measured with an American Perkin-Elmer-Lamda 900 UV/VIS/NIR spectrophotometer. Upconversion luminescence measurements were performed by a 976 nm LD pumping and a Triax-320 spectrophotometer detecting.

All the measurements were done at room temperature.

RESULTS AND DISCUSSION

Absorption Spectra

In the absorption spectra measured for all the samples shown in Fig. 1, it can be seen clearly that there are seven absorption bands, their absorption peaks centered at 486, 521, 546, 657, 808, 977, and 1533 nm, respectively. The energy levels diagram of Er^{3+}/Yb^{3+} is shown in Fig. 2, referring to W. T. Carnall's work [10], the data of the energy levels' wave-numbers were acquired from the absorption spectra. The seven absorption bands are corresponded to the transitions of $^4I_{15/2}(Er^{3+})\rightarrow{}^4F_{7/2}(Er^{3+})$, $^4I_{15/2}(Er^{3+})\rightarrow{}^2H_{11/2}(Er^{3+})$,$^4I_{15/2}(Er^{3+})\rightarrow{}^4S_{3/2}(Er^{3+})$, $^4I_{15/2}(Er^{3+})\rightarrow{}^4F_{9/2}(Er^{3+})$,$^4I_{15/2}(Er^{3+)}\rightarrow{}^4I_{9/2}(Er^{3+})$, $^4I_{15/2}(Er^{3+})\rightarrow{}^4I_{11/2}(Er^{3+})$ and $^2F_{7/2}(Yb^{3+})\rightarrow{}^2F_{5/2}(Yb^{3+})$, and$^4I_{15/2}(Er^{3+})\rightarrow{}^4I_{13/2}(Er^{3+})$. There exists the absorption peak at 977 nm, which is resonance absorption with 976 nm incident light. Therefore, we used 976 nm LD to pump the samples. Compared with the 977 nm absorption bands of Er^{3+} single doped material showing in Fig. 3, the corresponding absorption bands of Er^{3+}/Yb^{3+} co-doped matrix were more intense, this is because Er^{3+}/Yb^{3+} co-doped matrix has a larger absorption cross-section areas. As shown in Fig. 1a, the 977 nm absorption bands became more and more predominant in the sequence of TTK-1-*n* ($n = 1$, 2, 3, 4, 5, 6, 7, 8, 9, 10, and 11). That is to say, when the ratio of Yb^{3+}/Er^{3+} increases from 1/10 to 10/1, the

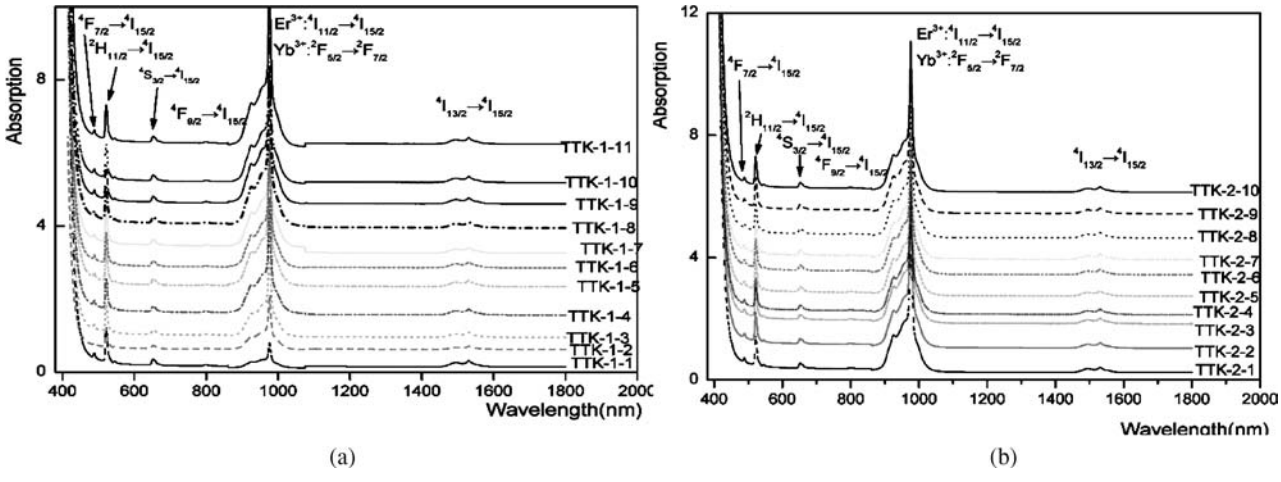

Fig. 1. The absorption spectra of the studied glasses. (a) TTK-1-*n* ($n = 1$, 2, 3, 4, 5, 6, 7, 8, 9, 10, and 11). (b) TTK-2-*n* ($n = 1$, 2, 3, 4, 5, 6, 7, 8, 9, and 10).

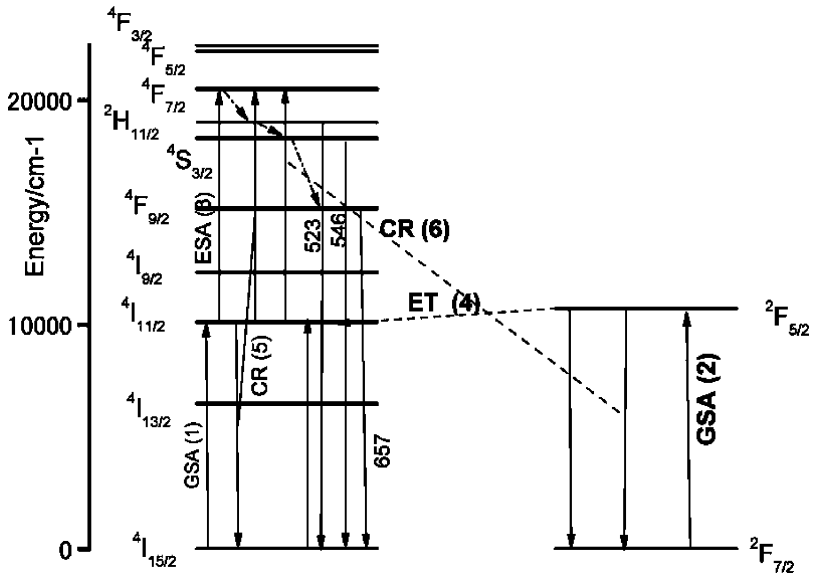

Fig. 2. The simple energy level diagram of Er^{3+}/Yb^{3+} co-doped TTK glasses.

977 nm absorption band gets more and more significant as the Er^{3+} concentration remains fixed; this is due to the transition of $^2F_{7/2}(Yb^{3+}) \rightarrow {}^2F_{5/2}(Yb^{3+})$ with high absorption efficiency. Taken TTK-1-10 and TTK-1-11 for an example, the absorption integral area (46.57 mm^2) and absorption peak height (1.414 mm) of TTK-1-11 are larger than those of TTK-1-10 (44.87 mm^2, 1.407 mm).

However, as for the absorption spectra of the TTK-2-n ($n = 1, 2, 3, 4, 5, 6, 7, 8, 9$, and 10) shown in Fig. 1b, no change can be detected in the 977 nm absorption bands. This is due to the saturation absorption of Yb^{3+}, as increasing the concentration of Yb^{3+} to some extent, the increasing absorption will be reach the saturation point, 1 mol% in our system.

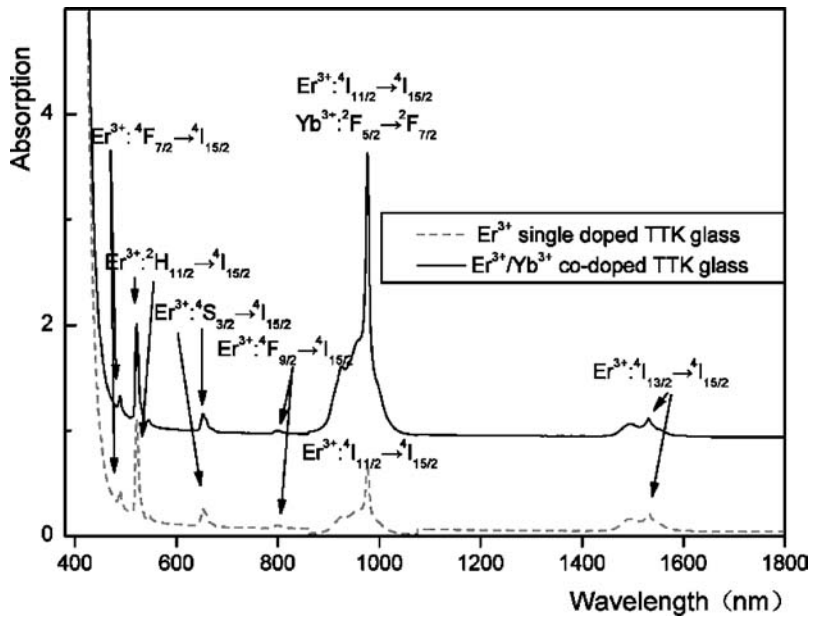

Fig. 3. The absorption spectra of Er^{3+}/Yb^{3+} co-doped TTK glasses is compared with that of Er^{3+} single doped TTK glasses.

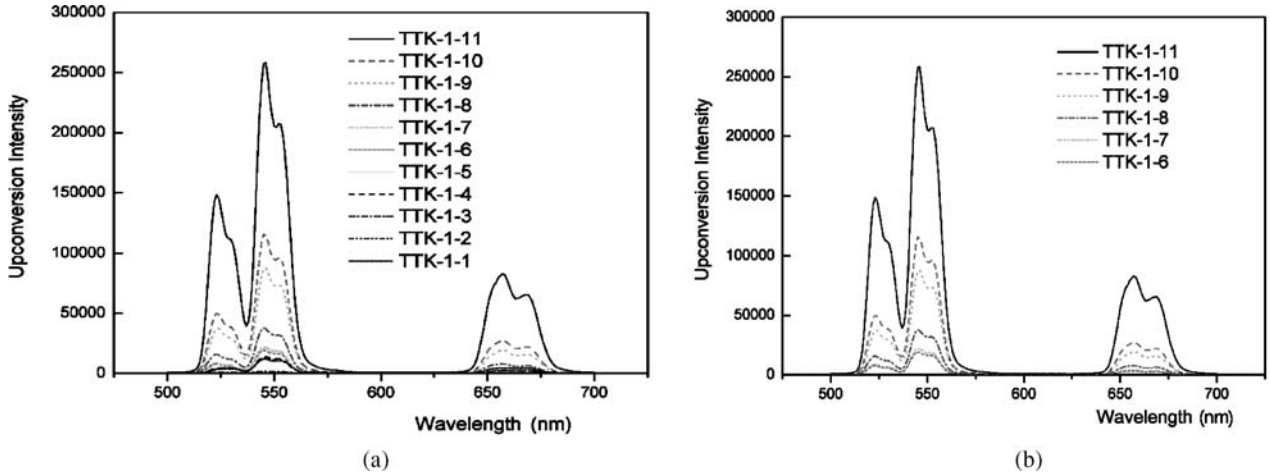

Fig. 4. Upconversion luminescence spectra of Er^{3+}/Yb^{3+} co-doped TTK-1-*n* glasses excited by 800 mW LD. (a) TTK-1-*n* ($n = 1, 2, 3, 4, 5, 6, 7, 8, 9, 10$, and 11). (b) TTK-1-*n* ($n = 6, 7, 8, 9, 10$, and 11).

Upconversion Spectra

The upconversion spectra of series I (TTK-1-n) are shown in Fig. 4. There are three emission bands in the visible light range, 523, 546, and 657 nm, respectively.

Figure 5 shows the intensity of 546 nm emission luminescence as a function of the excitation power, the plots are in log (I_{up}) versus log (I_{IR}). These results suggested that the $^2H_{11/2}$ level was populated by a two-photon steps process. The upconversion processes [8,11,12] can be described as below:

$$\text{GSA}: \quad {}^4I_{15/2}(Er^{3+}) + h\nu_0 \rightarrow {}^4I_{11/2}(Er^{3+}) \qquad (1)$$

$$ {}^2F_{7/2}(Yb^{3+}) + h\nu_0 \rightarrow {}^2F_{5/2}(Yb^{3+}) \qquad (2)$$

$$\text{ESA}: \quad {}^4I_{11/2}(Er^{3+}) + h\nu_0 \rightarrow {}^4F_{7/2}(Er^{3+}) \qquad (3)$$

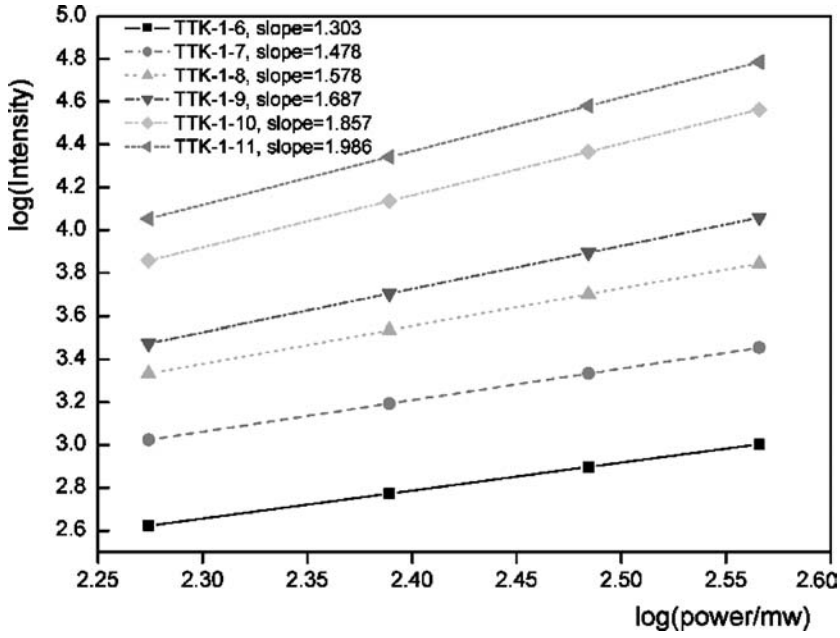

Fig. 5. The 546 nm upconversion luminescence intensity of TTK-1-*n* ($n = 6, 7, 8, 9, 10$, and 11) VS pump power. The plot is in log (I_{up}) vs. log (I_{IR}).

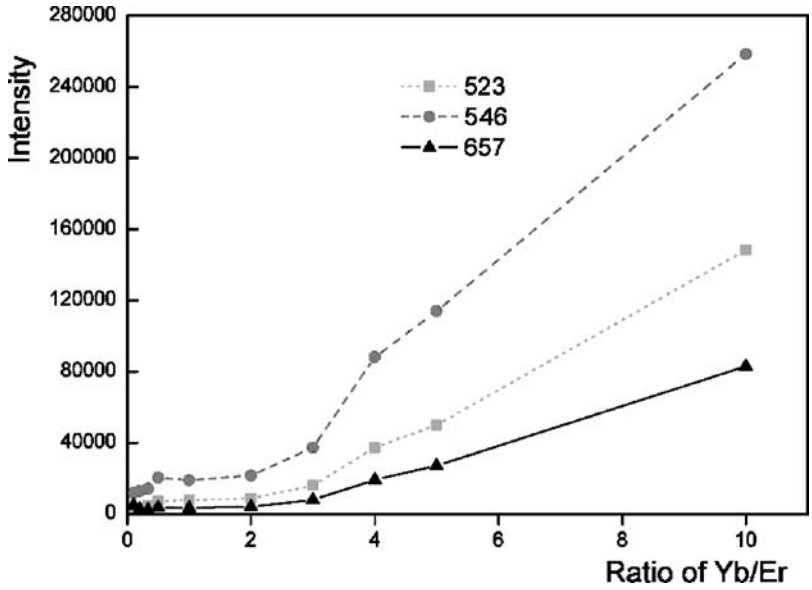

Fig. 6. The dependence of upconversion luminescence intensity on *R* (presentation for ratio of Yb^{3+}/Er^{3+}).

$$\text{ET}: \quad {}^2F_{5/2}(Yb^{3+}) + {}^4I_{15/2}(Er^{3+}) \rightarrow {}^2F_{7/2}(Yb^{3+}) + {}^4I_{11/2}(Er^{3+}) \tag{4}$$

$$\text{CR}: \quad {}^4I_{11/2}(Er^{3+}) + {}^4I_{11/2}(Er^{3+}) \rightarrow {}^4F_{7/2}(Er^{3+}) + {}^4I_{15/2}(Er^{3+}) \tag{5}$$

$$ {}^2F_{5/2}(Yb^{3+}) + {}^4I_{11/2}(Er^{3+}) \rightarrow {}^2F_{7/2}(Yb^{3+}) + {}^4F_{7/2}(Er^{3+}) \tag{6}$$

As discussed in Section Absorption Spectra, the absorption at 977 nm of Yb^{3+} gets more and more predominant with increasing ratio of Yb^{3+}/Er^{3+}. This means that the ET (energy transfer) mechanism will be more dominant, that is to say, the process [Eqs. (2), (4), and (6)] will be more dominant when the ratio of Yb^{3+}/Er^{3+} increases. Referred to Fig. 2 (the above-mentioned process are all marked in Fig. 2), due to the resonate absorption at 976 nm, Yb^{3+} strongly absorbed the incident photons of 976 nm LD, a Yb^{3+} ion rose from ground state ${}^2F_{7/2}$ to the excited state ${}^2F_{5/2}$, then the excited Yb^{3+} transferred its' energy to Er^{3+} by ET (4) process as Eq. (4), thus caused the Er^{3+} ion to excite from its' ground state ${}^4I_{15/2}$

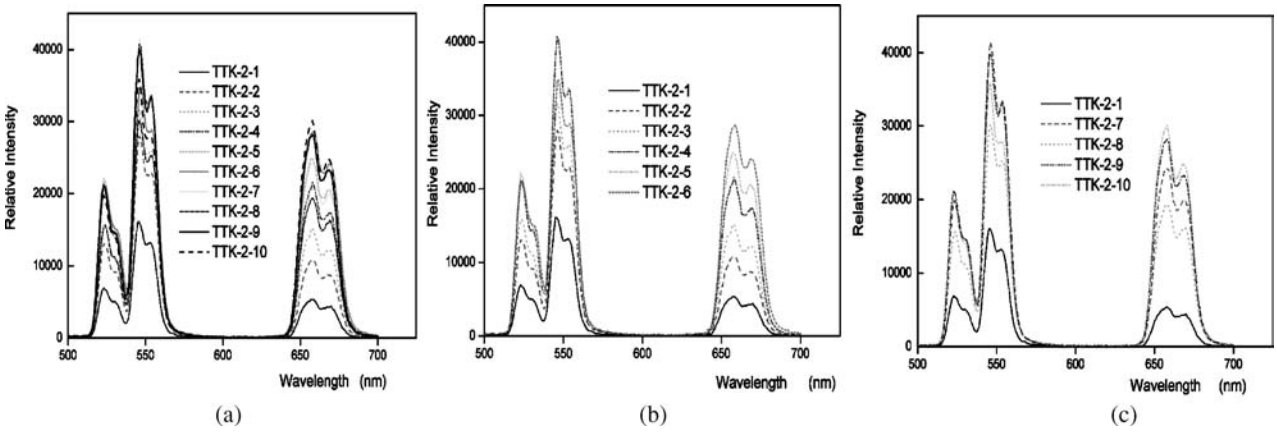

Fig. 7. Upconversion luminescence spectra of Er^{3+}/Yb^{3+} co-doped TTK-2-*n* glasses excited by 490 mW LD. (a) TTK-2-*n* ($n = 1, 2, 3, 4, 5, 6, 7, 8, 9$, and 10); (b) TTK-2-*n* ($n = 1, 2, 3, 4, 5$, and 6); and (c) TTK-2-*n* ($n = 1, 7, 8, 9$, and 10).

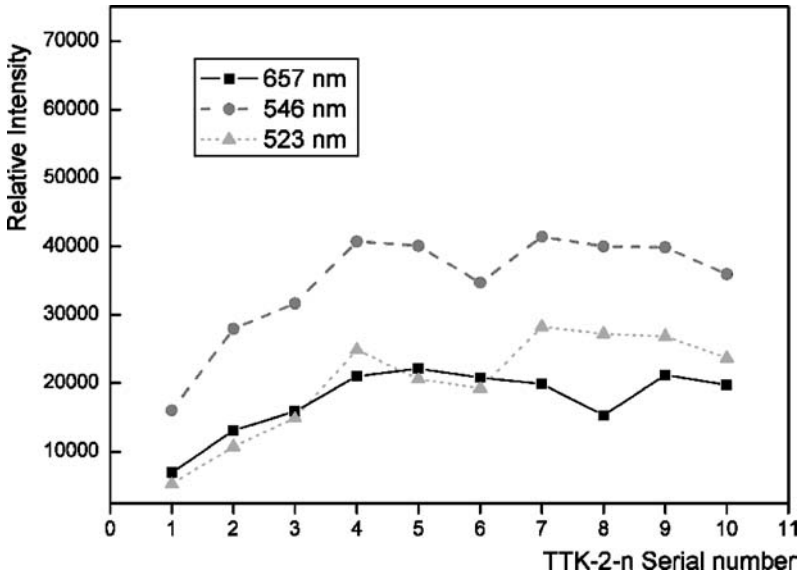

Fig. 8. Dependence of upconversion luminescence intensity on Yb^{3+}/Er^{3+} ratio and Er^{3+} concentration. There are two maximum, TTK-2-4 and TTK-2-7.

to the excited state $^4I_{11/2}$, the Er^{3+} ion in$^4I_{11/2}$ could be further excited to$^4F_{7/2}$ through the CR (6) process. Since the life-time of the Er^{3+} ions at $^4F_{7/2}$ level is too short, it relaxes rapidly to the $^2H_{11/2}$ via non-radioactive transition. Similarly, those Er^{3+} ions at $^2H_{11/2}$ level may also non-radioactively relax to $^4S_{3/2}$ level, and then the Er^{3+} ions at$^4S_{3/2}$ level would non-radioactively relax to $^4F_{9/2}$ level. When the ions in $^2H_{11/2}$ level radiate relax to the ground level $^4I_{15/2}$, they emit the 523 nm green luminescence; similarly, the ions in level$^4S_{3/2}$,$^4F_{9/2}$ relax to the ground level $^4I_{15/2}$, they respectively emit 546 and 657 nm upconversion luminescence.

The relationship between the upconversion luminescence intensity and the ratio of Yb^{3+}/Er^{3+} are shown in Fig. 6; the 523, 546, and 657 nm emission intensities increase as R increases. Especially, from TTK-1-6 to TTK-1-11, the upconversion luminescence intensity increase rapidly with increasing R. From Figs. 4b and 6, the increasing trend is obvious.

In order to get the optimal Er^{3+} concentration and Yb^{3+}/Er^{3+} ratio for the potential application in microchip solid-state lasers, Series II experiments were carried out. The upconversion spectra of TTK-2-*n* are shown in Fig. 7. Figure 7b shows the dependence of upconversion intensities on R, where the concentrations of Er^{3+} were fixed at 0.1 mol% for all samples from TTK-2-1 to TTK-2-6. The 546 nm upconversion peak intensities were in the order: TTK-2-1 < TTK-2-2 < TTK-2-3 < TTK-2-6 < TTK-2-5 < TTK-2-4. From the experiment the maximum intensity was obtained around $R = 25/1$ in our studied glass system.

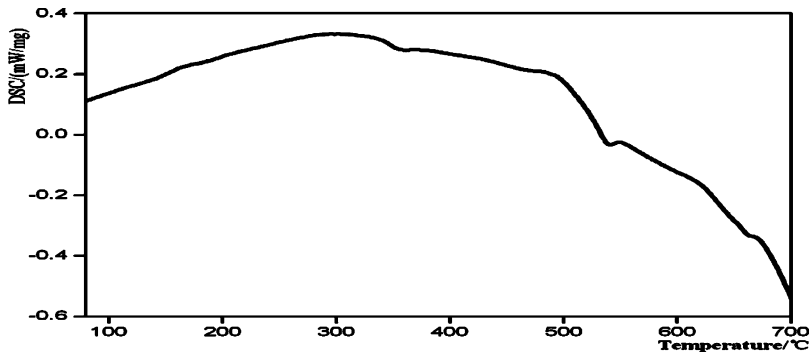

Fig. 9. The DSC curve of TTK-2-7.

The explanation of the above phenomenon can be given as: The Yb^{3+} concentration will increase as R increases, and the so-called concentration quenching [13] of Yb^{3+} would happen; therefore, the energy transfer will be restricted by some concentration limit, which induces the upconversion luminescence decrease.

The relationship between upconversion intensity and Er^{3+} concentration are clearly shown in Fig. 7c, where all samples (TTK-2-1, TTK-2-7, TTK-2-8, TTK-2-9, and TTK-2-10) were set to $R = 10/1$, it revealed the upconversion intensity order: TTK-2-1 < TTK-2-10 < TTK-2-9 < TTK-2-8 < TTK-2-7. The phenomenon can be interpreted as follows: As concentration of Er^{3+} increases, the Er^{3+} ions play the main role in determining upconversion luminescence intensity. While the Er^{3+} concentration increases to some extent, Er^{3+}–Er^{3+} interaction will happen. This interaction will transfer their energy in thermal form, thus lower luminescence intensity. This is so-called concentration quenching.

The maximum of the upconversion intensity was obtained from two ways shown in Fig. 8; one is fixing Er^{3+} concentration at 0.1 mol% and changing the Yb^{3+}/Er^{3+} ratio, TTK-2-4; the other is fixing the Yb^{3+}/Er^{3+} ratio at $R = 10/1$ and changing Er^{3+} concentration, TTK-2-7. The two maximum intensities are very close in quantity in our work.

In order to meet the application need of the studied material, the thermal quality of TTK-2-7 was also studied, according to Fig. 9, there is no crystalline peak in the whole thermal process. That is to say, the thermal quality of TTK-2-7 is excellent.

CONCLUSIONS

The absorption spectra and upconversion spectra of Er^{3+}/Yb^{3+} co-doped TTK glasses are measured and discussed. The dependence of upconversion luminescence intensity on the Er^{3+} concentration and the ratio of Yb^{3+}/Er^{3+} are studied in detail. The optimal upconversion intensity can be obtained either when the Yb^{3+}/Er^{3+} ratio is 25/1 and Er^{3+} concentration is 0.1 mol%, or when the Yb^{3+}/Er^{3+} ratio is 10/1 and Er^{3+} concentration is 0.15 mol%. The intense green upconversion luminescences were observed in all the samples with naked eyes, which announce their potential application advantage in the field of LD pumping microchip solid-state lasers.

ACKNOWLEDGMENTS

This work was supported by Science and Technology Program of Guang Zhou, Guangdong province, PR China (Grant NO. 2004Z2-D0131 and 2004A10602002), National Natural Science Foundation of China (Grant NO. 60307004 and 50472053), and Natural Foundation of Guangdong Province, PR China (Grant NO. 04200036).

REFERENCES

1. S. X. Dai, J. H. Yang, S. Q. Xu, N. L. Dai, L. Wei, L. L. Hu, and Z. H. Jiang (2003). Multi-rare-earth ions co-doped tellurite glasses for potential dual wavelength fibre-optic amplifiers. *Chin. Phys. Lett.* **20**(1), 130–132.
2. D. C. Yeh, W. A. Sibley, M. Suscavage, and M. G. Drexhage (1987). Multi-phonon relaxation and infrared-to-visible conversion of Er^{3+} and Yb^{3+} ions in barium–thorium fluoride glass. *J. Appl. Phys.* **62**(1), 266–275.
3. T. Ohta, M. Takenaga, N. Akahira, and T. Yamashita (1982). Thermal changes of optical properties observed in some sub-oxide thin films. *J. Appl. Phys.* **53**(**12**), 8497–8500.
4. M. Takenaga, N. Yamada, K. Nishiuchi, N. Akahira, T. Ohta, and S. Nakamura (1983). TeO_x thin films for an optical disc memory. *J. Appl. Phys.* **54**(9), 5376–5380.
5. M. F. A. Kuhaili, S. M. A. Durrani, E. E. Khawaja, and J. Shirokoff (2002). Effect of preparation conditions on the optical properties of thin films of tellurium oxide. *J. Phys. D Appl. Phys.* **35**, 910–915.
6. F. N. Su, Z. D. Deng, and Z. H. Jiang (2005). Research progress of upconversion tellurite fiber lasers. *Gong neng cai liao* **36**(5), 655–657 (in Chinese).
7. Li-Yan Zhang, Jian-Hu Yang, Li-Li Hu, and Zhong-Hong Jiang (2003). High efficiency infrared to visible upconversion in Er^{3+}/Yb^{3+}-doped lead halide tellurite glass. *Chin. Phys. Lett.* **20**(8), 1344–1346.
8. Zhong-Min Yang, Shi-Qing Xu, Li-Li Hu, and Zhong-Hong Jiang (2004). Energy transfer and frequency upconversion in Yb^{3+}/Er^{3+} co-doped sodium–lead germinate glasses. *J. Alloys Compds.* **370**, 94–98.
9. Zheng-Wei Liu, Hui-Xian Yang, Xiao-Liang Yang, Fang-Cheng Yuan, and Si-Guo Xiao (2003). Study on the upconversion mechanism of Yb^{3+} *Spectrosc. Spect. Anal.* **23**(5), 846–848 (in Chinese).
10. W. T. Carnall, P. R. Fields, and K. Rajnak (1968). Electronic energy levels in the trivalent lanthanide ions IPr^{3+}, Nd^{3+}, Pm^{3+}, Sm^{3+}, Dy^{3+}, Ho^{3+}, Er^{3+} and Tm^{3+}. *J. Chem. Phys.* **49**, 4424–4442.
11. F. Vetrone, J. C. Boyer, J. A. Capobianco, A. Speghini, and M. Bettinelli (2004). Significance of Yb^{3+} concentration on the upconversion mechanisms in co-doped Y_2O_3:Er^{3+}/Yb^{3+} nano-crystals. *J. Appl. Phys.* **96**(1), 661–667.
12. Jian-Hu Yang, Neng-Li Dai, Shi-Xun Dai, Lei Wen, Li-Li Hu, and Zhong-Hong Jiang (2003). Enhancement of upconversion luminescence in Er^{3+} doped tellurite glasses due to the introduction of $PbCl_2$. *Chem. Phys. Lett.* **376**, 671–675.
13. Y. G. Choi, B. J. Park, and K. H. Kim (2002). Ho^{3+}: $({}^5S_2, {}^5F_4) \rightarrow {}^5I_5$ transition in fluoride glasses. *Chem. Phys. Lett.* **354**(1–2), 69–74.